Hydrogen Bonding Properties of Oxygen and Nitrogen Acceptors in Aromatic Heterocycles

I. NOBELI,[1] S. L. PRICE,[1] J. P. M. LOMMERSE,[2] R. TAYLOR[2]

[1] *University College London, Department of Chemistry, 20 Gordon Street, London WC1H 0AJ, United Kingdom*

[2] *Cambridge Crystallographic Data Centre, 12 Union Road, Cambridge CB2 1EZ, United Kingdom*

Received 27 January 1997; accepted 4 August 1997

ABSTRACT: The directionality and relative strengths of hydrogen bonds to monocyclic aromatic heterocycles were investigated using crystal structure data and theoretical calculations. Surveys of the Cambridge Structural Database for hydrogen bonds between $C^{(sp3)}$—O—H and aromatic fragments containing one or more nitrogen and/or oxygen heteroatoms showed that hydrogen bonds to nitrogen atoms are much more abundant than to oxygen. Distinct preferred orientations were also revealed in these surveys. Theoretical calculations were performed on the interaction of methanol with pyridine, pyrimidine, pyrazine, pyridazine, oxazole, isoxazole, 1,2,4-oxadiazole, and furan as models for the heterocyclic fragments. The intermolecular potential surface was thoroughly scanned using a model potential that accurately described the electrostatic forces (derived from distributed multipole analysis) with empirical parameters for the repulsion and dispersion terms. Minima on this surface agreed well with the observed orientations in the data base and they were typically deeper for nitrogen than for oxygen acceptors, although the hydrogen bond strength and geometry was influenced by other heteroatoms in the ring. These results were confirmed by highly accurate intermolecular perturbation theory calculations, which also estimated the deviations from hydrogen bonding in the traditional nitrogen lone pair direction that could occur with negligible reduction in the interaction energy. *J Comput Chem* **18**: 2060–2074, 1997

Keywords: hydrogen bond; Cambridge Structural Database (CSD); distributed multipole analysis (DMA); intermolecular perturbation theory (IMPT); heterocycle

Correspondence to: S. L. Price; E-mail: s.l.price@ucl.ac.uk

Contract/grant sponsor: EPSRC; contract/grant number: GR/J31865

CCC 0192-8651 / 97 / 162060-15

Introduction

An understanding of the relative strengths and geometries of intermolecular contacts, such as hydrogen bonds, is required for the design of new supramolecular materials, including the engineering of crystal structures, or for selecting functional group replacements in protein ligands to enhance binding affinity. In biological systems, the prevalence of N and O suggests that replacing an oxygen with a nitrogen acceptor in a ligand could retain the hydrogen bond to the protein and yet produce a chemically distinct ligand. This requires a knowledge of the relative strengths and directional requirements of the hydrogen bond acceptors.

Aromatic heterocycles containing nitrogen and oxygen are common organic compounds that often form part of protein ligands. The effect on binding of substitution of one heterocycle for another in a ligand will crucially depend on the relative acceptor strengths of the heteroatoms. Recent studies[1] of the hydrogen bonding capabilities of oxygen atoms covalently bonded to an sp^2 hybridized atom showed that these were often considerably weaker acceptors than equivalent nitrogen atoms. This is in contrast to the common expectation, based solely on electronegativity, that both are good acceptors. Because some oxygen heterocycles were shown to be weak acceptors in that study, we undertook a study of the relative hydrogen bonding strengths for the common heterocycles furan, pyridine, 1,2-oxazole (isoxazole), 1,3-oxazole (oxazole), pyrimidine, pyrazine, pyridazine, and 1,2,4-oxadiazole.

A good source of experimental information on the geometries of hydrogen bonds is the Cambridge Structural Database.[2] Where there are a statistically significant number of hydrogen bonds to a heterocycle in the data base, any commonly observed geometry is likely to correspond to a strong interaction and the scatter of geometries indicates the variation in geometry caused by the steric limitations of the crystal packing of the wide range of bonded functional groups. Conversely, if hydrogen bonds are rarely found in crystal structures containing the heterocycle and a hydrogen bond donor, then this suggests that the hydrogen bond is weak, at least relative to the other interactions that stabilize the crystal structures.

Whereas experimental crystal structure determinations provide statistical probabilities of hydrogen bond geometries over a wide range of molecular environments, such analyses do not quantify the strength of the interaction or explain it. Therefore, we also performed theoretical studies on the interaction of methanol with each heterocycle to determine how the strength of the hydrogen bond varies with the acceptor and other heteroatoms in the ring. Methanol was chosen as the simplest single hydrogen bond donor, and so the results complement previous self-consistent field–second-order Møller–Plesset (SCF-MP2) supermolecule calculations on water hydrogen bonded to oxazole, isoxazole, and furan[1] because water is a very different, possibly bidentate, O—H donor. The aim was to determine the range of favorable hydrogen bonding geometries and understand the reason for the variation in hydrogen bond strength, rather than to determine a precise minimum energy structure for a given molecular pair. Hence, we used an approximate model intermolecular pair potential for surveying the potential energy surface, supplemented by intermolecular perturbation theory[3–5] (IMPT) calculations of each of the major contributions to the interaction energy at a limited range of geometries. This combination of crystal structure analysis with intermolecular energy calculations on model systems proved to be very powerful in providing a quantitative understanding of Cl···Cl,[6] halogen–oxygen, and halogen–nitrogen contacts,[7] contrasting with the hydrogen bonding properties of carbonyl, ether, and ester oxygen atoms[8] and accounting for asparagine–arginine,[9] water–phenylalanine,[10] amino–aromatic,[11] and other interactions between protein fragments.[12]

The electrostatic contribution to the intermolecular forces, which is the classical Coulombic interaction between the undistorted charge distributions of the molecules, dominates the intermolecular interaction at long range and generally determines the orientation dependence of the intermolecular potential in the van der Waals contact region. This was shown by the ability of an accurate (distributed multipole representation of *ab initio* molecular charge distributions) electrostatic plus hard-sphere repulsion model potential to predict the geometries of over 24 hydrogen bonded van der Waals complexes.[13] Thus, in this study a distributed multipole electrostatic model was used for scanning the methanol–heterocycle potential energy surface.

Hydrogen bond energy has significant contributions from the other intermolecular forces present. The additional interactions at the long range are

the induction (polarization) that arises from the distortion of the charge distribution of each molecule caused by the electrostatic field of the other molecules and the dispersion energy arising from the correlation of instantaneous electron density fluctuations within the molecules. When there is a significant overlap of the molecular charge distributions, the exchange energy describing the energetically favorable exchange of electrons of parallel spin between the two molecules is dominated by the repulsion energy arising from the Pauli exclusion principle. The charge-transfer energy, the result of excitations of electrons from occupied orbitals of one molecule to virtual ones of the other, is another short-range contribution, which gives a slight covalency to the hydrogen bond. The long-range forces are also modified by the onset of overlap in an exponential form. The exponentially decaying short-range net repulsive forces balance the long-range attractive forces in determining the minimum energy length of the hydrogen bond. All these contributions can be calculated by IMPT[3–5] applied to the SCF wave functions of the isolated molecules without any basis set superposition, although the division between the charge transfer and polarization energy is basis set dependent. Such calculations using a moderate basis set (6-31G**) have been shown[14] to give intermolecular interaction energies that have a good linear correlation with MP2 supermolecule calculations using a triple ζ polarized (TZP) basis set for a wide range of small organic molecules and for a large variety of hydrogen bonded systems. IMPT calculations have the advantage of providing a clearer insight into the intermolecular interaction because the various contributions are calculated separately, but the disadvantage is that geometry optimization of the dimer is difficult.

The crystal structure analysis and theoretical calculations both show that the hydrogen bond accepting ability of oxygen atoms in an aromatic ring is significantly less than for carbonyl, ether, or ester oxygens, or for heterocyclic nitrogen atoms. The hydrogen bonds are weaker, less likely to be linear (O—H···O), and more widely scattered around the X—O—X bisector in the molecular plane. Thus, substituting oxygen for nitrogen heterocycles will generally have a marked effect on the binding of a protein ligand, although this and other interactions will be modified by other heteroatoms in the ring.

Methods

Information on crystal structure data was retrieved from the Cambridge Structural Database[2] (CSD, version 5.11, April 1996, 152,464 entries). X-ray and neutron diffraction studies were both included in the study, and the poorly determined hydrogen positions from X-ray experiments were normalized so that the X—H distance would equal 1.083, 1.009, and 0.983 Å for C—H, N—H, and O—H, respectively. (These are the average values[15] from neutron diffraction experiments.) QUEST 3D[16] software was used to search the CSD for intermolecular hydrogen bonds between the H—O—C^{T4} (T4 indicates a tetrahedral sp^3 hybridized carbon) atom fragment and aromatic fragments representing the heterocyclic molecules in this study. The length of the hydrogen bond was accepted as anything up to the sum of the van der Waals radii for the hydrogen and the acceptor atom, where the radii are 1.52 Å[17] for oxygen, 1.55 Å[17] for nitrogen, and 1.09 Å[18] for the hydrogen. An interaction was rejected when the angle α (O—H···A, where A is the acceptor) was smaller than 90°, because this can no longer be considered as a hydrogen bond. To improve the quality of the CSD searches some secondary criteria were used. Only crystal structures with R factors < 0.1 with no errors in the coordinates and no disorder were accepted, and polymeric structures were excluded. Organic and organometallic compounds were both included in the search. The results for the various geometric descriptors of the hydrogen bond (see Fig 1) were graphically analyzed using VISTA.[19]

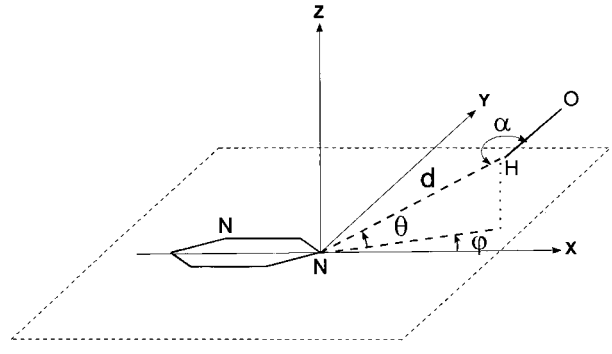

FIGURE 1. Definition of the hydrogen bond geometrical parameters: the hydrogen bond length (N/O···H), d; the angle at the proton (N/O···H—O), α; the in-plane deviation from the ideal nitrogen lone pair direction, φ; and the out of plane deviation from the ideal nitrogen lone pair direction, θ.

For the theoretical calculations, the geometry of each model molecule was optimized at the MP2 level of theory and with a 6−31G** basis set, using the program CADPAC.[20]

Because a thorough scanning of the potential surface around each heterocycle was needed, we had to use a model potential, which would be computationally inexpensive but would still give a reasonably accurate description of the most important interactions and would reflect as well as possible the directionality of the hydrogen bond. Electrostatic interactions are of great importance in van der Waals hydrogen bonded dimers[21] and the orientation dependence of the electrostatic energy profile closely parallels that of the total energy one,[22] so an accurate representation of the electrostatic forces combined with empirical isotropic atom−atom functions for the other major contributions can be expected to give a reasonably good description of the intermolecular surface, particularly the orientation dependence. The electrostatic interactions were calculated from the sets of atomic multipoles obtained by a distributed multipole analysis (DMA)[23,24] of the MP2 6−31G** monomer wave function, including all terms in the multipole expansion up to R^{-5}. The model potential, U_{ik}, also includes 6-*exp* repulsion and dispersion terms, that is,

$$U_{ik} = A_{\iota\kappa}\exp(-B_{\iota\kappa}R_{ik}) - \frac{C_{\iota\kappa}}{R_{ik}^6} + U_{ik}(\mathrm{DMA}, R_{ik}^{-n}, n \le 5),$$

where the atoms i and k are of type ι and κ; and the parameters B, A, and C are those of Williams and Cox[25] for C, H, and N and Cox et al.[26] for O. For hydrogen atoms directly bonded to nitrogen or oxygen, the repulsion-dispersion parameters were fitted to hydrogen bonded crystal structures.[27] This model potential was used to scan the methanol−heterocycle potential energy surface by starting minimizations at a sufficient variety (20−40) of orientations (using the ORIENT[28] program), so it seemed highly probable that all significant minima were found.

The single point *ab initio* calculations of the total interaction energy were performed using the IMPT[3−5] code of CADPAC at the 6−31G** level. IMPT calculations yield at first order the electrostatic (E_{es}) and exchange−repulsion (E_{er}) terms, and at second order the charge transfer (E_{ct}), polarization (E_{pol}), and a series of double excitation terms from which only the dispersion energy (E_{disp}) was considered in this study because the other terms are spurious.

Results

RESULTS FROM CSD SEARCHES

Table I summarizes the number of hydrogen bonds found in our surveys of the CSD. Because the number of hydrogen bonds involving C^{T4}—O—H donors is large for only pyridine and pyrimidine, searches were also performed with a less restrictive definition of the donor, using any C—O—H or O—H fragments. A search for N—H donors to 1,2,4-oxadiazole is also included in Table I, because no hydrogen bonds were found involving oxygen donors to this heterocycle.

Nitrogen Versus Oxygen Acceptors in CSD

As Table I reveals, there are relatively more hydrogen bonds to nitrogen than to oxygen atoms in aromatic heterocycles. For example, there are 126 unique crystal structures containing a pyridine ring and the H—O—C^{T4} fragment, and in 64 of these there is a hydrogen bond to the nitrogen atom. In the case of a furan ring the corresponding numbers are 71 and 1. The 3-dimensional plot of hydrogen donors around the nitrogen and the oxygen in isoxazole (represented in Fig. 2) shows that nitrogen is clearly the preferred acceptor when there is direct competition in the crystal. These results are in agreement with the recent study of Böhm et al.[1] They found a dramatically larger amount of hydrogen bonds to nitrogen acceptors than to oxygen when the N or O atom is bonded to at least one sp^2 hybridized atom.

Geometry of the Hydrogen Bond in CSD

There is a strong preference for near-linear hydrogen bonds to the nitrogen atoms of pyridine and pyrimidine, and the vast majority of hydrogen bonds have α values greater than 155° (47 out of 64 for pyridine and 66 out of 84 for pyrimidine). A similar preference for linearity was seen in the hydrogen bonds to the other nitrogens. However, the few hydrogen bonds to aromatic oxygens in heterocyclic systems are far from linear; all the hydrogen bonds have α values lower than 155°, and the majority of them have α values lower than 140°.

TABLE I.
Results from CSD Searches.

	Donor Fragment					
	H—O—C^{T4}		H—O—C		H—O	
Heterocycle	HBOND	TOT	HBOND	TOT	HBOND	TOT
Pyridine	64	126	116	246	174	322
Pyrimidine	84	115	100	135	128	159
Pyrazine	4	8	7	20	13	24
Pyridazine	1	2	1	3	5	6
Oxazole (N)	2	4	5	8	6	8
Oxazole (O)	0	4	0	8	0	8
Isoxazole (N)	2	4	5	15	11	20
Isoxazole (O)	1[a]	4	1[a]	15	3[a]	20
1,2,4-Oxadiazole (N2)	0	0	0	0	0	2
1,2,4-Oxadiazole (O)	0	0	0	0	0	2
1,2,4-Oxadiazole (N4)	0	0	0	0	0	2
Furan	1	71	2	98	7	119
Tetrahydrofuran	149	823	161	851	202	878
Dihydrofuran	4	33	4	39	6	40

	N—H donors	
	HBOND	TOT
1,2,4-Oxadiazole (N2)	5	12
1,2,4-Oxadiazole (O)	0	12
1,2,4-Oxadiazole (N4)	1	12

TOT, number of unique REFCODES containing both the donor and heterocyclic fragments; HBOND, number of these TOT structures that contain at least one donor–heterocycle hydrogen bond. T4 implies tetrahedral carbon.
[a] These hydrogen bonds satisfy the criteria for being hydrogen bonded to both the nitrogen and the oxygen atoms, but are closer to the nitrogen.

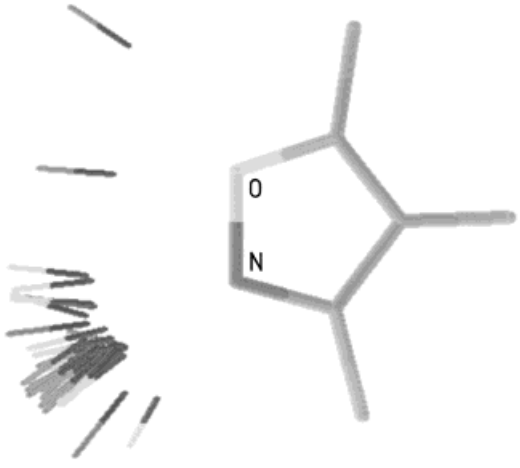

FIGURE 2. The scatter of O—H and N—H groups around the isoxazole fragment, as retrieved from the Cambridge Structural Database. The plot shows all contacts of polar hydrogens with the O or N, which are less than 2.42 and 2.45 Å, respectively.

The two CSD searches for which there are enough data for a θ-φ scattergram (Fig. 3a, b) show a distinct preference for the hydrogen bond to form in the plane and direction of the nitrogen lone pair. For both cases of pyridine and pyrimidine fragments the majority of the hits lie within 20° of the plane of the ring ($|\theta| \leq 20°$) and within 20° ($|\varphi| \leq 20°$) from the direction of the x axis[29] (which coincides with the idealized lone pair direction). The hydrogen bond geometries for pyrazine (Fig. 3c) and the N acceptor of isoxazole (Fig. 3d) follow similar trends, although the data is much more limited. In the majority of other cases of nitrogen acceptors, the value of θ does not exceed 20°. Similarly, the angle φ is generally limited to values less than 20°. There is significant φ asymmetry in the distributions for pyrimidine and isoxazole.

The number of hydrogen bonds to oxygen acceptors is so small that the results are not statisti-

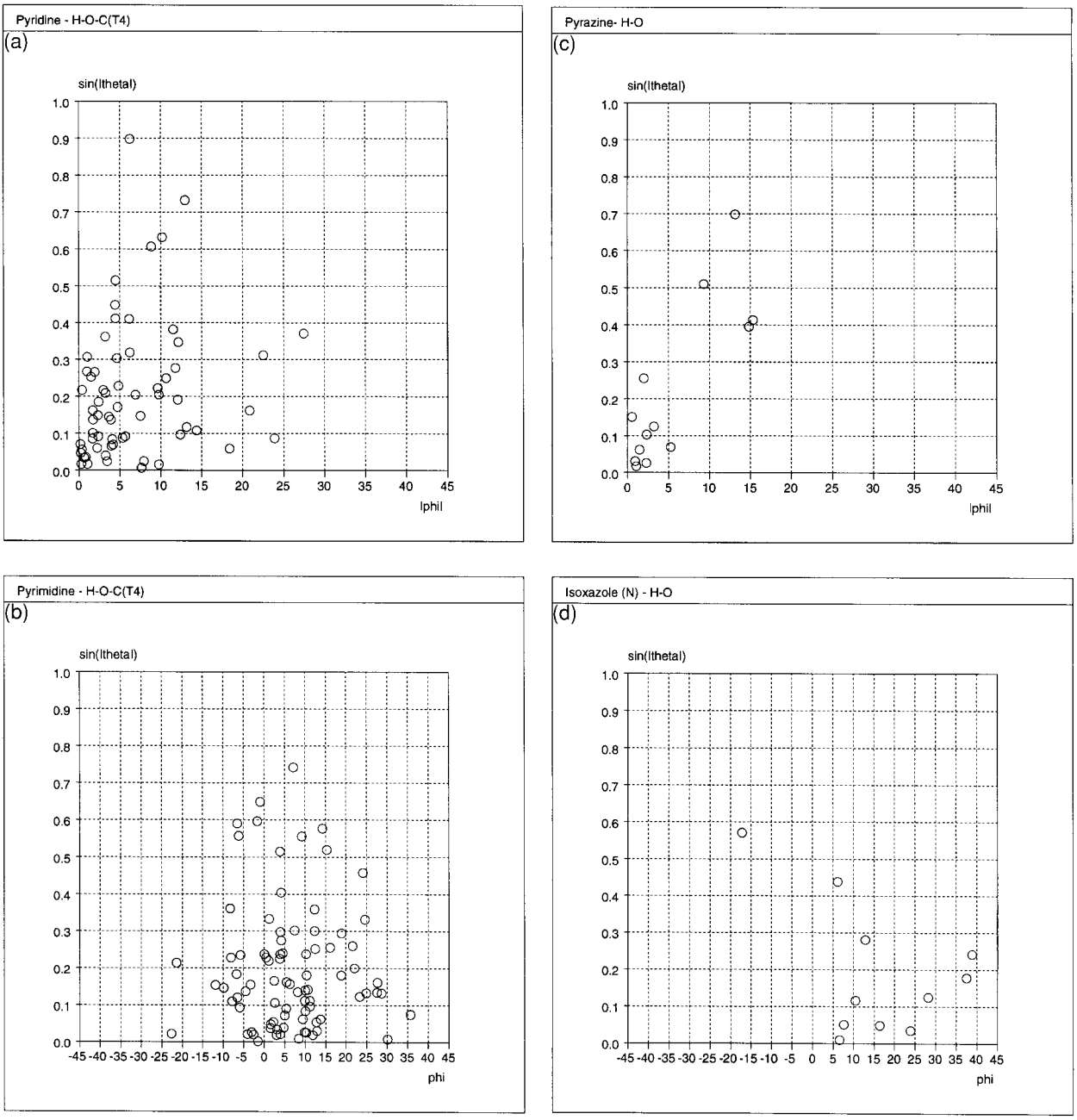

FIGURE 3. Scatter plots of sin θ vs. φ values (see Fig. 1 for the definition of these angles) for (a) the pyridine$\cdots$H—O—C^{T4}, (b) pyrimidine$\cdots$H—O—C^{T4}, (c) pyrazine$\cdots$H—O, and (d) isoxazole (N)$\cdots$H—O hydrogen bonded dimers retrieved from the CSD. The sine of θ is used so that equal areas on the diagram correspond to equal volumes of space.[8]

cally meaningful. However, the θ and φ angles are similar to the ones observed for nitrogen acceptors. Only in the case of the one hydrogen bond involving an H—O—C^{T4} donor, θ is much larger (43°).

All these trends agree with past research on similar hydrogen bonded complexes, where strong directionality preferences have been observed for hydrogen bonds to sp^2 nitrogens.[30–32]

RESULTS FROM THEORETICAL CALCULATIONS

Using Model Potential

The search for minima in the DMA + 6-*exp* potential energy surface of each heterocycle being probed by a methanol molecule resulted in the

minima pictured in Figure 4, where both the DMA + 6-*exp* estimates (in parentheses) and the more accurate IMPT energies at the same geometries are reported. Their energies confirm that in general hydrogen bonds to heterocyclic nitrogen are more stable than those to heterocyclic oxygen, with the possible exception of the N2 and O of 1,2,4-oxadiazole.

The minimum energy methanol–heterocycle structures correspond to the most common hydrogen bond geometries in the CSD searches. The hydrogen bonds to nitrogen are much more linear than the ones to oxygen acceptors. In all but one (1,2,4-oxadiazole N4) case, the bonds to the nitrogen atoms have $\alpha > 170°$, whereas the corresponding values for the bonds to oxygen atoms vary from 115° to 151°. The θ angle is very small (in all cases smaller than 5°), with again the largest deviations from the plane of the ring being in the case of oxygen acceptors. In all cases of asymmetrical environments around the acceptors, the in-plane deviations (in φ) are larger than the out of plane deviations in θ. In the nitrogen acceptors in symmetrical environments (pyridine and pyrazine), φ is zero as expected; that is, the donor proton is approaching in the direction traditionally assigned to an sp^2 nitrogen lone pair. For the unsymmetrical nitrogen acceptors, φ deviates from zero by a few degrees. These small deviations from the idealized lone pair direction are away from a second nitrogen, but toward an oxygen in the same ring. Deviations from $\varphi = 0°$ are much larger and less predictable for oxygen acceptors. Even in the symmetric case of furan, where the oxygen is the only heteroatom in the ring, the hydrogen bond is at $|\varphi| = 16°$, and the methanol O is even further displaced from the C^{sp2}—O—C^{sp2} bisector toward the hydrogen on the α carbon.

The potential energy surfaces of methanol with pyridine, pyrimidine, isoxazole (N), and pyrazine were contoured as a function of θ and φ for fixed separation and optimized methanol orientation (CH_3O—). The plots for pyridine, pyrazine, and isoxazole (Fig. 5a) are in agreement with the experimental distributions (Fig. 3a, c, d); the low energy regions correspond to the largest population of hydrogen bond geometries. (In all cases, over 95% of the total CSD hydrogen bonded structures are within 10 kJ/mol of the minimum.) This is illustrated for isoxazole where both the energy contours and the data base scatter plots show a mild preference for positive φ angles (i.e., a preference for hydrogen bonding on the side of the oxygen). The plot for pyrimidine is an exception; Figure 5b has the lowest energy contour that is slightly displaced toward negative φ angles, whereas the experimental distribution (Fig. 3b) is skewed to positive φ. The discrepancy seems to be related to the fact that the most common form of hydrogen bonded pyrimidine in the data base has a five membered ring fused with the pyrimidine ring at the 5 and 6 position and an NHR substituent at the 4 carbon, which will sterically hinder hydrogen bonds at negative φ. This is borne out by the percentage of pyrimidine rings fused to five or six membered rings and hydrogen bonded to H—O—C^{T4}. Only 66% of the hydrogen bonds with negative φ correspond to fused rings, but between $\varphi = 0°$ and $\varphi = 20°$, 92% are fused. All hydrogen bonds with φ greater than 20° correspond to fused pyrimidine rings. This is additionally confirmed by the unfused pyrimidine rings showing the trend predicted by the DMA + 6-*exp* calculations (9 out of 12 have negative φ).

IMPT Calculations

To obtain a better estimate of the energies calculated with the model potential, we initially performed IMPT calculations on all hydrogen bonded minima using the DMA + 6-*exp* minimum energy geometries. The results are reported in Figure 4. Comparing these to the DMA + 6-*exp* energies (numbers in parentheses), we observe that the stability of hydrogen bonds to nitrogen was consistently overestimated (by ~ 1.5–6 kJ/mol), whereas that of the bonds to oxygen was underestimated (by ~ 1–4 kJ/mol), probably due to the inaccuracy of the isotropic empirical parameters in the model potential. However, the overall result, that most of the aromatic oxygens are significantly weaker acceptors than the nitrogens, was confirmed.

IMPT calculations were subsequently performed for all methanol-heterocycle combinations at comparable geometries, based on the idealized values: $\theta = 0°$, $\varphi = 0°$, and $d = 1.85$ Å. Each time one of the three was varied: the distance d between the proton and the acceptor, the angle φ, or the angle θ. In all cases, the angle α was fixed at 180°. Figure 6 summarizes the results for pyridine and furan.

The striking feature in Figure 6 is the flatness of the potential with variation in the separation d. The variation in the total energy is in all cases less than 3.4 kJ/mol for a change of 0.25 Å (from $d = 1.85$–2.10 Å) in the H···N/O distance, and in most cases it is actually no more than 2.0 kJ/mol

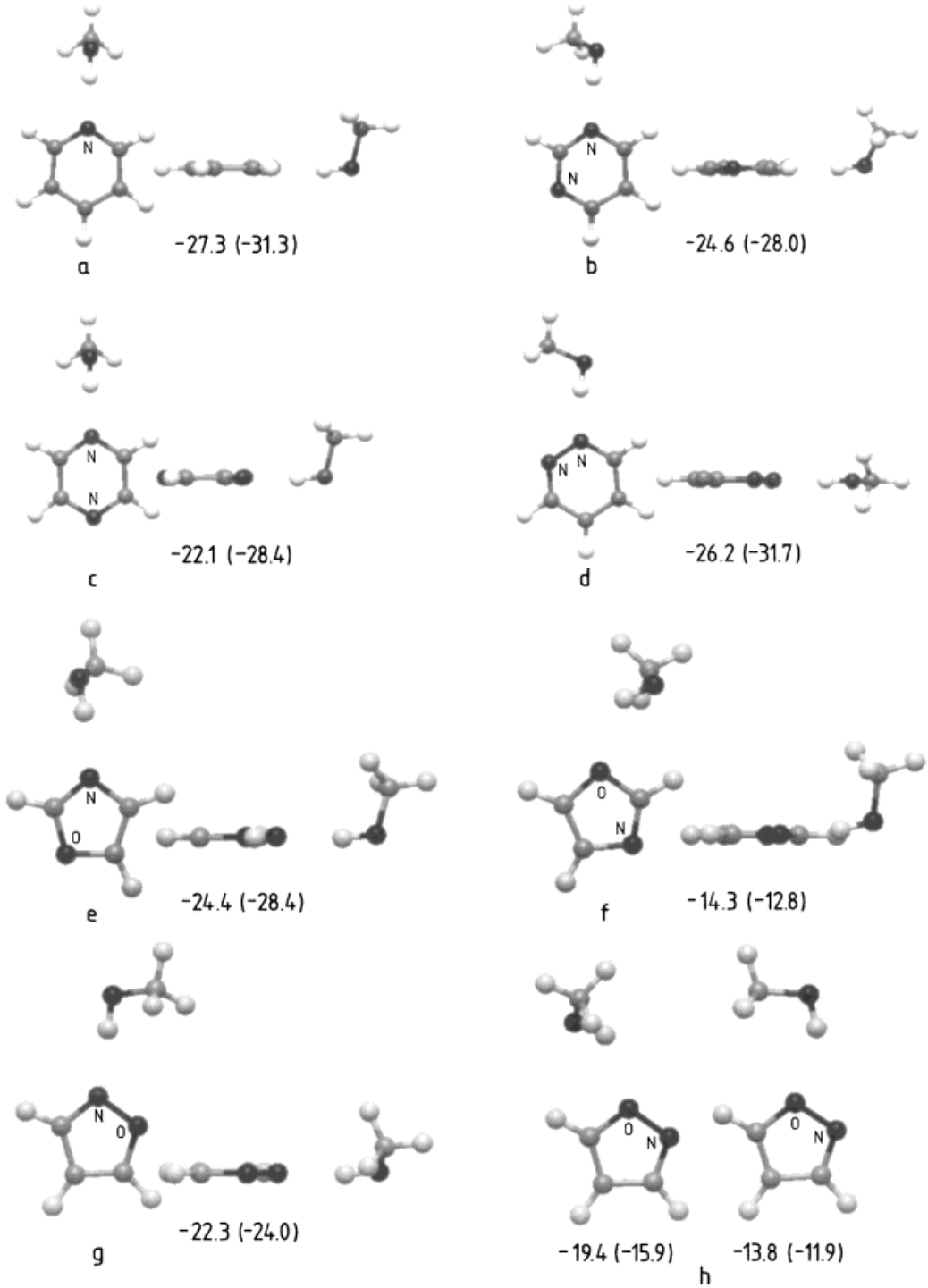

FIGURE 4. Geometry of the most important minima in the model potential for heterocycle$\cdots$methanol and the corresponding IMPT total intermolecular energies (the DMA + 6-*exp* energies are also given in parentheses). Two different views are shown for each dimer, except the two isoxazole minima. Other minima involving the methanol oxygen as acceptor or with the donor proton pointing to the π system have not been included. (a) Pyridine, (b) pyrimidine, (c) pyrazine, (d) pyridazine, (e) oxazole (N), (f) oxazole (O), (g) isoxazole (N), (h) isoxazole (O), (i) 1,2,4-oxadiazole (N2), (j) 1,2,4-oxadiazole (N4), (k) 1,2,4-oxadiazole (O), and (l) furan.

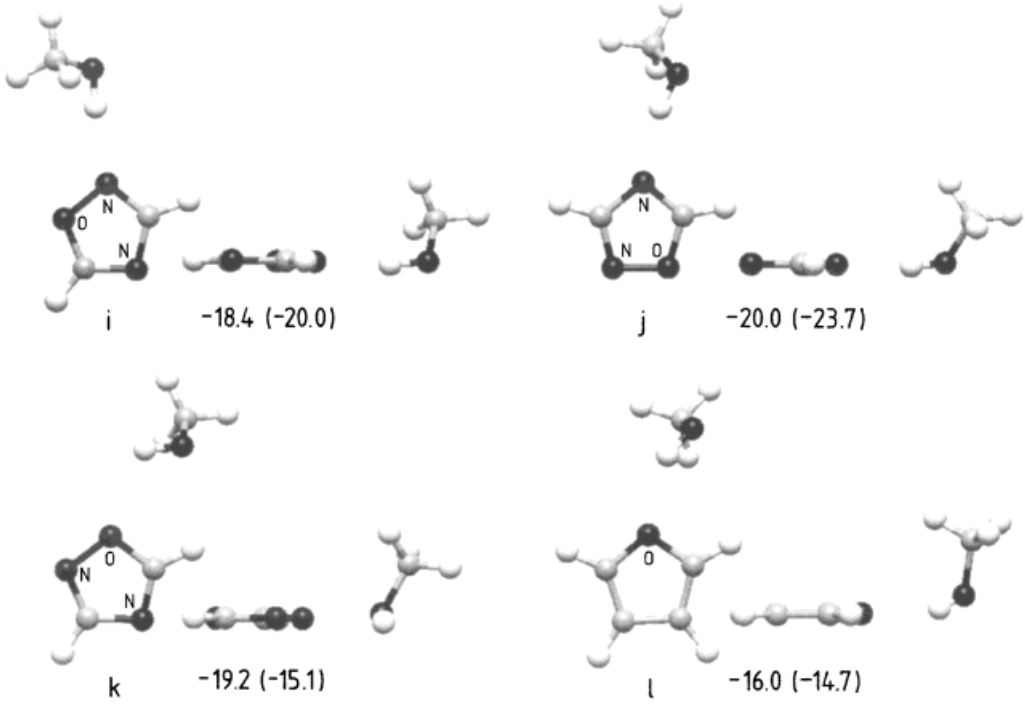

FIGURE 4. (Continued)

(a larger variation in energy being for N2 and O of 1,2,4-oxadiazole). In the case of $\theta = 0°$ and $\varphi = 0°$, the minimum energy orientation for the interaction between pyridine and methanol is at a distance d (from the proton to the nitrogen acceptor) of 1.95 Å, whereas the minimum for the furan case is at $d = 2.0$ Å (d was increased in steps of 0.05 Å). For the remaining heterocycles the optimum values for d vary between 1.95 and 2.10 Å, and the contacts involve oxygen acceptors having the same or slightly higher optimum d values as compared with the contacts to nitrogen acceptors.

IMPT calculations performed at $d = 1.85$ Å and $\theta = 0°$ for the in-plane angle φ varying in steps of 10° show that in the majority of cases the minimum in the interaction is at $\varphi = 0°$, that is, in the direction traditionally assigned to the nitrogen lone pair. The exceptions are contacts to N and O of isoxazole and N2 and O of 1,2,4-oxadiazole, where the minimum is at $\varphi = +10°$. Thus, this result agrees in sign with the observed trend in the CSD. The variation of the energy of interaction on either side of the minimum is dependent on the environment of the acceptor atom. For a change of 20°, the largest change in energy observed is for the N2 acceptor of 1,2,4-oxadiazole (4.7 kJ/mol), but the majority of cases show a change in energy of less than 2.5 kJ/mol. Comparing nitrogen and oxygen acceptors in the same ring, the potential seems to be flatter around oxygen than around nitrogen atoms. For example, in oxazole, the energy of the $H\cdots N$ contact changes by 2.5 kJ/mol on moving the donor proton from $\varphi = 0°$ to $\varphi = 20°$, whereas the corresponding change for the oxygen acceptor in the same molecule is 1.9 kJ/mol.

Finally, IMPT calculations performed at constant d and φ and varying out of plane angle θ show (in all cases) a minimum for the energy of interaction with methanol at $\theta = 0°$. The area of minimum interaction energy corresponds then to the area of the nitrogen lone pair, in or near the plane of the ring. However, the energy of interaction is reduced by 10 kJ/mol only for θ values greater than 40°, and changes in energy corresponding to a deviation of 20° from $\theta = 0°$ are not larger than 3.1 kJ/mol. If only oxygen acceptors are considered, this number is smaller than 0.7 kJ/mol, which shows that the potential around

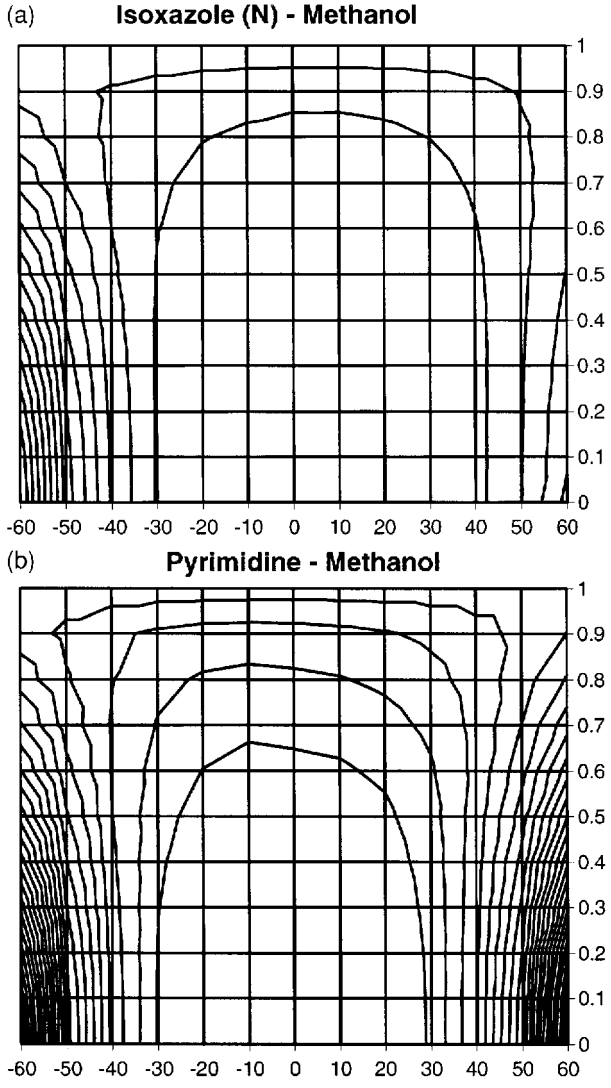

FIGURE 5. Contour diagrams for the variation of the energy of interaction between (a) isoxazole (N) with a methanol molecule (minimum at -24.0 kJ / mol, innermost contour line at -20 kJ / mol, further contours at increasing energy by 5 kJ / mol) and (b) pyrimidine (minimum at -27.3 kJ / mol, innermost contour line at -25 kJ / mol, further contours at increasing energy by 5 kJ / mol) for $d = 1.95$ Å and a series of φ and θ angles. The DMA + 6-*exp* calculations were performed using the constrained minimization code of ORIENT. The aromatic ring had its position and orientation fixed, and the methanol molecule was free to change its orientation with only the position of the proton being constrained to a point. The points chosen were the grid points of the VISTA $\sin(\theta)$-φ scattergrams, with values for the $\sin(\theta)$ varying from 0.0 to 1.0 in steps of 0.1 and values for φ varying from $-60°$ to 60° in steps of 10°. The results of these calculations are plotted in 2 dimensions, and the contour lines showing the depth of the potential are directly comparable with the experimental distributions (Fig. 3).

these oxygen atoms (in the plane perpendicular to the plane of the aromatic ring) is flatter than the potential around the nitrogen acceptors.

Discussion

NITROGEN VERSUS OXYGEN: COMPETITION FOR HYDROGEN BONDS

The data base searches indicate that the hydrogen bonds to nitrogens largely outnumber those to oxygens, a surprising result considering that these two atoms have been long thought to have similar abilities for accepting protons. However, a recent study of the CSD by Böhm et al.[1] agrees well with our observations, and thus it seems that the old view[33] that correlates the electronegativity of an atom with its ability to form hydrogen bonds must be treated with caution. In this case then, we are left with the question of what determines the relative abilities of atoms to accept protons. We noted here that the electrostatic potential around the pyridine nitrogen is a factor greater than two more negative than that around the furan oxygen (-171.4 and -74.3 kJ/mol, respectively, at a distance of 1.90 Å from the acceptor), and thus it correlates well with the proton accepting abilities of these two atoms.

Theoretical calculations support the conclusions drawn from the CSD searches and allow generalizations where there are only a few hits. IMPT calculations at the ORIENT minimized geometries confirmed that differences of 5–10 kJ/mol are common between hydrogen bonds to nitrogen and those to oxygen. However, the minimum energy geometries for the heterocyclic oxygen–methanol complexes deviate significantly from the idealized hydrogen bond geometries, as will be discussed later. IMPT calculations at comparable geometries further emphasized these conclusions. In all, oxazole, isoxazole, and 1,2,4-oxadiazole hydrogen bonds to nitrogen are typically more stable than the ones to oxygen by over 6 kJ/mol, over a range of H···A distances (1.75–2.15 Å, for $\theta = 0°$ and $\varphi = 0°$). Very similar results are obtained when the hydrogen bond length is kept constant and the angles φ or θ are changed over a range of values. This is in agreement with the high quality supermolecule calculations performed by Böhm et al.[1] on selected hydrogen bonded complexes showing a difference of approximately 10 kJ/mol between geometrically optimized dimers involving sp^2 nitrogens and those involving sp^2 oxygen atoms. In

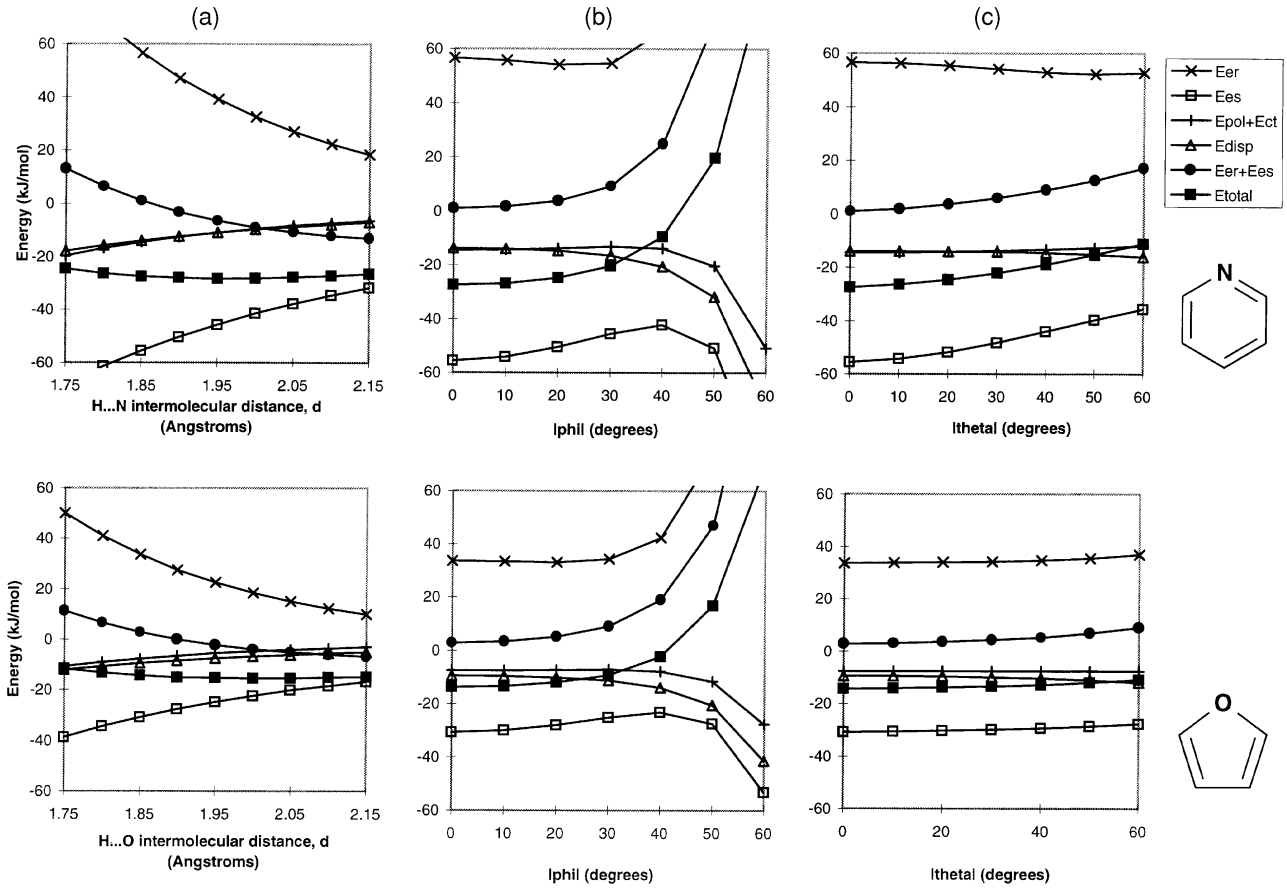

FIGURE 6. The variation of the energy of interaction (from the IMPT calculations) between (top) pyridine and methanol and (bottom) furan and methanol with (a) H···N intermolecular distance, (b) φ, and (c) θ, starting from $d = 1.85$ Å, $\varphi = 0°$, $\theta = 0°$, $\alpha = 180°$, and the CH_3 group in the plane perpendicular to the heterocycle and varying only the specified variable. The sum of the charge transfer and polarization terms is reported, as the two become indistinguishable at the basis set limit.

addition, it became evident from our study that neighboring atoms in the ring could significantly affect the stability of the bond. For example, in 1,2,4-oxadiazole, there is only a marginal difference between the energy of the hydrogen bonds to N4 (−20.0 kJ/mol) and O (−19.2 kJ/mol); the latter is actually slightly lower than that of the bond to N2 (−18.4 kJ/mol).

It is evident that in most cases there is good correlation between the theoretically calculated energy of a hydrogen bond and the probability for it to appear in the data base when there are a significant number of observations. The only exception is 1,2,4-oxadiazole that has five N—H hydrogen bonds to N2, one to N4, and none to oxygen, although the minimum energy calculations for methanol suggest that the three heteroatoms are equally good acceptors. A possible explanation is that the majority of 1,2,4-oxadiazole rings in our search are 3,5 substituted. This makes N4 less sterically accessible and also destabilizes hydrogen bonds to O by removing the attractive interaction with the 5 hydrogen (see Fig. 4k and later discussion).

A comparison of the IMPT calculations for the pyridine–methanol and furan–methanol complexes offers an insight into the origin of the difference between the stabilities of the two. The pyridine–methanol complex is over 11 kJ/mol more stable than the furan–methanol one over a broad range of H···O distances (1.75–2.15 Å). Comparing the contributions to the total energy (Table II) at $d = 1.95$ Å (the minimum energy separation for pyridine) and $d = 2.00$ Å (for furan), it is clear that the total difference in stabilities remains more or less the same but the balance of contributions

changes. The stronger attractive forces in pyridine produce more overlap at its minimum energy separation (1.95 Å) and hence stronger repulsion, so the sum of the first-order terms only favors pyridine by 4.2 kJ/mol. The dispersion and the sum of charge transfer and polarization also favor pyridine by comparable amounts. At the larger separation found in furan, pyridine is still favored and the electrostatic term makes a larger contribution. Again all terms significantly favor pyridine. Thus, the stronger electrostatic forces in pyridine lead to a shorter optimum hydrogen bond distance and a greater overlap of the charge distributions and hence a larger magnitude for all terms.

To confirm that these results are not just an artifact of comparing N and O, we note that comparable IMPT minimum energy for the tetrahydrofuran–methanol dimer is −25.3 kJ/mol (i.e., comparable with pyridine) at $d = 1.95$ Å, $\theta = 0°$, and $\varphi = 0°$. There are also a large number of tetrahydrofuran rings hydrogen bonded to H—O—C[T4] fragments in the CSD (149 out of 823). At the tetrahydrofuran minimum for $\varphi = 0°$ and $\theta = 0°$ ($d = 1.85$ Å) and the furan minimum ($d = 2.0$ Å), the difference in the electrostatic energies of the two complexes accounts for over 80% of the difference in the total energies. We are currently investigating[34] the reduced electrostatic contribution in the furan case compared with phenol, anisole, and tetrahydrofuran.

EFFECT OF OTHER HETEROATOMS IN RING

Theoretical calculations using the model DMA + 6-*exp* potential and IMPT show that the energy of a hydrogen bond to an sp^2 nitrogen or oxygen is significantly affected by the neighboring atoms in the ring.

Among the six membered rings, pyridine undoubtedly forms the strongest hydrogen bonds for a range of H···N distances and θ and φ angles. Similarly, the pyrazine nitrogens are the poorest hydrogen bond N acceptors, forming complexes that are approximately 5 kJ/mol less stable than the pyridine ones. Pyrimidine and pyridazine are involved in hydrogen bonds of intermediate stability. The difference between the pyrimidine and the pyridazine dimers is typically less than 1 kJ/mol, and pyrimidine complexes are marginally more stable at low values of d (< 1.95 Å). The differences observed are mainly due to the electrostatic term that shows the most significant variation among the six membered heterocycles.

Looking now at the five membered rings with at least one nitrogen acceptor, we see that the oxazole nitrogen is affected by the presence of the oxygen at the β position and compared to the pyridine nitrogen, it forms hydrogen bonds to methanol that are approximately 3 kJ/mol less stable over a range of d values. All contributions to the total energy are smaller in magnitude than

TABLE II.
The Total Energy of Interaction and the Various Contributions as Calculated Using IMPT.

Energy Terms (kJ / mol) from IMPT	Pyridine–Methanol		Furan–Methanol		Difference (Furan–Pyridine)	
	$d = 1.95$ Å	$d = 2.0$ Å	$d = 1.95$ Å	$d = 2.0$ Å	$d = 1.95$ Å	$d = 2.0$ Å
E_{es}	−45.6	−41.4	−24.8	−22.3	20.8	19.1
E_{er}	39.2	32.5	22.5	18.4	−16.6	−14.1
E_{pol} (total)	−5.2	−4.6	−2.7	−2.3	2.5	2.3
Ring	−2.3	−2.1	−1.6	−1.4	0.8	0.7
Methanol	−2.8	−2.5	−1.1	−0.9	1.7	1.6
E_{ct} (total)	−5.7	−4.9	−2.9	−2.4	2.8	2.5
Ring → methanol	−4.0	−3.4	−1.9	−1.6	2.1	1.8
Methanol → ring	−1.7	−1.5	−0.9	−0.8	0.8	0.7
E_{disp}	−10.9	−9.7	−7.6	−6.8	3.3	2.9
E (first order)	−6.4	−8.9	−2.2	−3.9	4.2	5.0
E_{total}	−28.2	−28.1	−15.3	−15.4	12.9	12.7

Values are for the pyridine–methanol and furan–methanol dimers at intermolecular distances (d) of 1.95 Å and 2.0 Å. Both calculations are at $\theta = 0°$, $\varphi = 0°$, $\alpha = 180°$, and with the CH_3 group in the plane perpendicular to the heterocycle.

those of the pyridine complex. Moreover, an oxygen at the α position (as in the isoxazole case) has an even bigger effect. The total intermolecular energy of the isoxazole nitrogen interacting with the methanolic oxygen at 1.95 Å ($\varphi = \theta = 0°$) is only −21.0 kJ/mol (cf. the corresponding energy for pyridine is −28.2 kJ/mol, and for oxazole is −25.1 kJ/mol). In the case of 1,2,4-oxadiazole, the results are as expected for a combination of nitrogen and oxygen neighbors. N2 is the weakest hydrogen bond acceptor of all the nitrogens we studied (−16.8 kJ/mol at 1.95 Å), because it has both an oxygen at the α position and a nitrogen at the β. N4 is slightly better (−19.9 kJ/mol at the same geometry), but it is still very much affected by the presence of the two other heteroatoms at the β positions.

Turning our attention to oxygen acceptors, the stability of hydrogen bonds to methanol (for d = 2.0 Å and $\varphi = \theta = 0°$) decreases as we go from furan (−15.4 kJ/mol) to isoxazole (−14.2 kJ/mol), then to oxazole (−11.6 kJ/mol), and finally to 1,2,4-oxadiazole (−10.0 kJ/mol). This order remains the same for a range of distances d and angles θ and φ. Thus, in this case again, the presence of a nitrogen in the ring destabilizes the bond, primarily through worse electrostatic interactions. Furthermore, a nitrogen at the β position has a bigger effect on the acceptor oxygen than one at the α position. These conclusions can be contrasted with the IMPT energies of the DMA + 6-*exp* minima. All such minima involving oxygen acceptors have more favorable IMPT energies than any of the idealized geometries. For furan this difference is marginal, but for the other heterocycles it is significant. Figure 4 reveals that in all cases the oxygen of methanol is displaced toward the ring, probably to maximize interactions with the α hydrogens. These α hydrogens (H_α) are in near van der Waals contact with the oxygen of methanol (O_{meth}). The $H_\alpha \cdots O_{meth}$ distances are for: oxazole, 2.75 Å (Fig. 4f), isoxazole, 2.74 Å (Fig. 4h); 1,2,4-oxadiazole, 2.61 Å (Fig. 4k); and furan, 3.07 Å (Fig. 4l). This results in the angle of the hydrogen bond α showing significant deviations from linearity (varying between 115° for 1,2,4-oxadiazole and 147° for furan). Hence, the geometry of the hydrogen bond is being significantly affected by the interactions between the hydrogen atom donor and the functional groups around the acceptor. Thus, the weaker hydrogen bonds to O show greater variation in geometry and strength because the additional interactions of the part of the model molecules not directly involved in the hydrogen bond are relatively more significant.

To assess relative energies we can rank the acceptors according to IMPT energies at d = 1.95 Å and $\theta = \varphi = 0°$:

pyridine (N, −28.2 kJ/mol) > oxazole (N, −25.2 kJ/mol), pyridazine (N, −25.1 kJ/mol), pyrimidine (N, −25.0 kJ/mol), pyrazine (N, −23.5 kJ/mol) > isoxazole (N, −21.0 kJ/mol), oxadiazole (N4, −19.9 kJ/mol) > oxadiazole (N2, −16.8 kJ/mol), furan (O, −15.3 kJ/mol) > isoxazole (O, −13.9 kJ/mol) > oxazole (O, −11.3 kJ/mol),
oxadiazole (O, −9.5 kJ/mol).

This ranking is similar over a range of distances d (1.95–2.05 Å). However, the ranking of the weaker acceptors will be much affected by the orientation and structure of the probe molecule, because these acceptors tend to distort more from the idealized geometry to optimize the interactions between other groups.

HYDROGEN BOND LENGTH VERSUS STRENGTH

The theoretical calculations predict that hydrogen bonds to pyridine or tetrahydrofuran are over 10 kJ/mol more stable than to the corresponding furan. The relative strengths of the hydrogen bonds of these heterocycles are reflected in the distances between the proton and the heteroatom in the CSD. Examining the hydrogen bonds between furan rings and H—O fragments (because there is only one hit for H—O—C^{T4}), one finds that there is no distance reported that is less than 2.1 Å (from a total of seven hits). For pyridine$\cdots$H—O interactions, there are 154 hits (out of 174) with hydrogen bond lengths shorter than 2.1 Å (88% of the total hits). For tetrahydrofuran$\cdots$H—O interactions, there are 153 hits (out of 202) with distances shorter than 2.10 Å (76%).

DIRECTIONALITY OF HYDROGEN BOND

The potential around an aromatic oxygen atom is flatter than the potential around an aromatic nitrogen (Fig. 6b top and bottom). For example, the H$\cdots$N interaction in the pyridine–methanol dimer is destabilized by 7.0 kJ/mol on going from $\varphi = 0°$ to $\varphi = 30°$, compared with a destabilization of 4.5 kJ/mol for the H$\cdots$O interaction in the

furan–methanol dimer (for $d = 1.85$ Å, but the trend is the same for $d = 2.0$ Å). In a crystal, where more interactions compete with the hydrogen bond, absolute values for the differences in energy with in and out of plane deviations from the direction of the ideal lone pair are important. Hence, in a crystal, contacts to oxygen acceptors will be more flexible in their geometry than those to nitrogens and a bigger scatter of θ and φ values can be expected for oxygen acceptors.

Our observation for the difference in flatness of the potential around aromatic nitrogen and oxygen acceptors agrees with previous studies on different types of oxygens. Lommerse et al.'s[8] IMPT calculations on the interaction of methanol with the oxygen acceptors in (*Z*)-methylacetate, methoxymethane, and propanone showed that in the plane of the oxygen lone pairs the potential does not change significantly for a wide range of angles. Mitchell and Price[35] used IMPT calculations on the formamide–formaldehyde complex to show the variation of the contributions to the energy with changes in the plane of the lone pair's angle; their plots showed a very flat profile for the total energy, which changed no more than 1 kJ/mol over a range of approximately 110° (corresponding to the region in space in between the two oxygen lone pairs). Apaya et al.[36] compared the DMA electrostatic potential around the formaldehyde oxygen and the histidine imidazole ND1 atoms and concluded that the potential around the oxygen is much flatter compared with the much sharper potential around nitrogen. For example, for moving 30° from the idealized lone pair direction, there was a change of 7.7 kJ/mol in the electrostatic potential around the nitrogen atom but only 0.2 kJ/mol in the potential around the oxygen.

In addition, IMPT calculations predict the distribution of the out of plane angles. The results show that if the energy is allowed to increase from its value at $\theta = 0°$ to any other value with a maximum increase of 5 kJ/mol, then in the vast majority of nitrogen acceptors the limit for the out of plane deviations (θ) would be 25°–35°. For oxygen acceptors, the scatter of θ values is bigger; a limit of over 50° is observed.

Conclusions

This study of hydrogen bonds to nitrogen and oxygen atoms in aromatic heterocyclic rings has shown that nitrogen is a significantly better proton acceptor than oxygen, and the furan aromatic oxygen is a much weaker acceptor than any of the oxygens in tetrahydrofuran, ester, ether, and carbonyl groups (with the exception of the etherlike oxygen in *Z*-methylacetate).[8] This fact is reflected in the much larger number of structures (retrieved from the CSD) having hydrogen bonds to nitrogen atoms, as compared with the corresponding number for hydrogen bonds to oxygen, especially when the two atoms are in a competitive situation (i.e., in the same ring).

The relative ordering of the total energies at comparable geometries roughly follows that of the electrostatic contribution. Stronger long-range attractive forces (which are predominantly electrostatic in hydrogen bonds) will displace the potential minimum slightly inward and be balanced by stronger repulsive forces, so all contributions tend to be larger in magnitude for the stronger total interactions. The observation that the weakness of the oxygen acceptors can be correlated with their weaker electrostatic interactions has significant implications for molecular modeling. The variation in strength of the hydrogen bonds to oxygen can only be represented by a force field whose electrostatic model reflects the charge distribution in the fragment, and not where the atomic charges are derived from electronegativities.

The study of the effect of neighboring atoms on the hydrogen bond acceptor revealed that the stability of the hydrogen bond to aromatic heterocycles is directly related to the environment of the acceptor. The energy of interaction of an H—O—C^{T4} fragment with an aromatic nitrogen is less favorable when a second nitrogen is introduced in the six membered ring, the destabilization being more dramatic in the case of a nitrogen at the para position than the ortho or meta. If the second heteroatom is oxygen (in a five membered ring), then the energy is again less negative; the effect is more pronounced for oxygens at the α position than for those at the β. For oxygen acceptors the situation is reversed: a nitrogen in the β position lowers the stability of the hydrogen bond to the oxygen more than a nitrogen at the α position does. All these observations seem to stem primarily from reduced electrostatic interactions.

The CSD searches suggest that hydrogen bonds to nitrogen and oxygen are formed primarily in the direction traditionally assigned to the nitrogen lone pair ($\theta = 0°$, $\varphi = 0°$), although there is some scatter of the θ/φ values. They also show a strong preference for linear or near-linear hydrogen bonds

to nitrogen acceptors and less linear contacts to oxygen acceptors. These observations are confirmed by the minima in energy obtained after a thorough scanning of the potential surface around each heterocycle with the use of a model DMA + 6-*exp* potential. Theoretical and statistical results both indicate that the sign of the φ angle is directly related to the presence of a second heteroatom in the ring. The IMPT calculations at comparable geometries show that the interaction between methanol and the various heterocycles has in all cases a rather flat minimum around $\varphi = 0°$, $\theta = 0°$, which explains the scatter observed in the data base. The potential seems to be slightly more flat for out of plane than for in-plane deviations from the position of the minimum.

The present research is part of an ongoing project to supplement the electronic library of nonbonded contact distributions in the CSD[37] with theoretical estimates of the relative strength and geometrical preferences of such intermolecular interactions. The combination of CSD surveys and theoretical studies of model compounds is a promising approach to the study of the interactions of organic molecules.

Acknowledgments

The computer resources were provided by EPSRC under Grant GR/J31865. I. N. gratefully acknowledges a CCDC studentship.

References

1. H. J. Böhm, S. Brode, U. Hesse, and G. Klebe, *Chem. Eur. J.*, **2**, 1509 (1996).
2. F. H. Allen and O. Kennard, *Chem. Design Automation News*, **8**, 1 (1993).
3. I. C. Hayes and A. J. Stone, *Mol. Phys.*, **53**, 83 (1984).
4. A. J. Stone, *Chem. Phys. Lett.*, **211**, 101 (1993).
5. A. J. Stone, *The Theory of Intermolecular Forces*, Clarendon Press, Oxford, 1996, chap. 6.
6. S. L. Price, A. J. Stone, J. Lucas, R. S. Rowland, and A. E. Thornley, *J. Am. Chem. Soc.*, **116**, 4910 (1994).
7. J. P. M. Lommerse, A. J. Stone, R. Taylor, and F. H. Allen, *J. Am. Chem. Soc.*, **118**, 3108 (1996).
8. J. P. M. Lommerse, S. L. Price, and R. Taylor, *J. Comput. Chem.*, **18**, 757 (1997).
9. J. B. O. Mitchell, C. L. Nandi, J. M. Thornton, S. L. Price, J. Singh, and M. Snarey, *J. Chem. Soc. Faraday Trans.*, **89**, 2619 (1993).
10. K. Flanagan, J. Walshaw, S. L. Price, and J. M. Goodfellow, *Protein Eng.*, **8**, 109 (1995).
11. J. B. O. Mitchell, C. L. Nandi, I. K. McDonald, J. M. Thornton, and S. L Price, *J. Mol. Biol.*, **239**, 315 (1994).
12. J. M. Thornton, M. W. MacArthur, I. K. McDonald, D. T. Jones, J. B. O. Mitchell, C. L. Nandi, S. L. Price, and M. J. J. M. Zvelebil, *Phil. Trans. R. Soc. Lond. A*, **345**, 113 (1993).
13. A. D. Buckingham and P. W. Fowler, *Can. J. Chem.*, **63**, 2018 (1985).
14. J. P. M. Lommerse, personal communication.
15. F. H. Allen, O. Kennard, D. G. Watson, L. Brammer, A. G. Orpen, and R. Taylor, *J. Chem. Soc. Perkin Trans.*, **2**, S1 (1987).
16. Cambridge Crystallographic Data Centre, *Cambridge Structural Database System Users Manual*, *Getting Started with the CSD System*, Cambridge Crystallographic Data Centre, Cambridge, U.K., 1994.
17. A. Bondi, *J. Phys. Chem.*, **68**, 441 (1964).
18. R. S. Rowland and R. Taylor, *J. Phys. Chem.*, **100**, 7384 (1996).
19. Cambridge Crystallographic Data Centre, *Cambridge Structural Database System Users Manual*, *Vista 2.0 Users Guide*, Cambridge Crystallographic Data Centre, 12 Union Road, Cambridge, U.K., 1996.
20. CADPAC5, *The Cambridge Analytic Derivatives Package*, Issue 5, University of Cambridge, Cambridge, U.K., 1992. This is a suite of quantum chemistry programs developed by R. D. Amos with contributions from I. L. Alberts, J. S. Andrews, S. M. Colwell, N. C. Handy, D. Jayatilaka, P. J. Knowles, R. Kobayashi, N. Koga, K. E. Laidig, P. E. Maslen, C. W. Murray, J. E. Rice, J. Sanz, E. D. Simandiras, A. J. Stone, and M.-D. Su.
21. H. Umeyama and K. Morokuma, *J. Am. Chem. Soc.*, **99**, 1316 (1977).
22. A. D. Buckingham, P. W. Fowler, and A. J. Stone, *Int. Rev. Phys. Chem.*, **5**, 107 (1986).
23. A. J. Stone, *Chem. Phys. Lett.*, **83**, 233 (1981).
24. A. J. Stone and M. Alderton, *Mol. Phys.*, **56**, 1047 (1985).
25. D. E. Williams and S. R. Cox, *Acta Crystallogr. B*, **40**, 404 (1984).
26. S. R. Cox, L.-Y. Hsu, and D. E. Williams, *Acta Crystallogr. A*, **37**, 293 (1981).
27. D. S. Coombes, S. L. Price, D. J. Willock, and M. Leslie, *J. Phys. Chem.*, **100**, 7352 (1996).
28. A. J. Stone, *ORIENT Version 3.2*, contributions from A. Dullweber, M. P. Hodges, P. L. A. Popelier, and D. J. Wales, University of Cambridge, 1996.
29. When statistical correction is applied, the range of θ values will be greater than that of φ, and so in the θ-φ scattergram, θ will look more scattered than φ.
30. A. Vedani and J. D. Dunitz, *J. Am. Chem. Soc.*, **107**, 7653 (1985).
31. A. L. Llamas−Saiz, C. Foces−Foces, O. Mo, M. Yañez, and J. Elguero, *Acta Crystallogr. B*, **48**, 700 (1992).
32. G. Klebe, *J. Mol. Biol.*, **237**, 212 (1994).
33. L. Pauling, *The Chemical Bond*, Cornell University Press, Ithaca, NY, 1967, p. 223.
34. I. Nobeli, S. L. Yeoh, S. L. Price, and R. Taylor, *Chem. Phys. Letts.*, to appear.
35. J. B. O. Mitchell and S. L. Price, *J. Comput. Chem.*, **11**, 1217 (1990).
36. R. P. Apaya, M. Bondi, and S. L. Price, *J. Comput.-Aided Mol. Design*, to appear.
37. I. J. Bruno, J. C. Cole, J. P. M. Lommerse, R. S. Rowland, R. Taylor, and M. L. Verdonk, *J. Comput.-Aided Mol. Design*, to appear.